Full Length Research Paper

Elastic stability of functionally graded rectangular plates under mechanical and thermal loadings

M. Bouazza[1,2]* and E. A. Adda-Bedia[2]

[1]Department of Civil Engineering, University of Bechar, Bechar 08000, Algeria.
[2]Laboratory of Materials and Hydrology (LMH), University of Sidi Bel Abbes, Sidi Bel Abbes 2200, Algeria.

In this paper, the buckling of a functionally graded plate is studied. The material properties of the plate are assumed to be graded continuously in the direction of thickness. The variation of the material properties follows a simple power-law distribution in terms of the volume fractions of constituents. The plates are subjected to be under three types of mechanical loadings, namely; uniaxial compression along the x-axis, uniaxial compression along the y-axis, and biaxial compression, two types of thermal loading, namely; uniform temperature rise and linear temperature rise. The equilibrium and stability equations are derived using the classical plate theory (Kirchhoff theory) and Navier's solution. Resulting equations are employed to obtain the closed-form solution for the critical buckling load for each loading case. The results are verified with the known data in the literature.

Key words: Buckling, classical plate theory, functionally graded materials, mechanical and thermal loads.

INTRODUCTION

In the recent studies on new performance, materials have addressed new materials known as functionally graded materials (FGMs). These are high performance and heat resistant materials able to withstand ultra high temperature and extremely large thermal gradients used in aerospace industries. Plates are one of the most important structures in engineering that are used widely in different fields. Buckling of plates especially plates made of functionally graded materials have been considered by engineers as a new field for researches, recently.

Buckling and postbuckling behaviors are one of the main interests in design of structural components such as plates, shells and panels for optimal and safe usage. Therefore, it is important to study the buckling and postbuckling behaviors of FGM plates under mechanical, thermal and combined thermo-mechanical loads for accurate and reliable design. Some works about the stability of FGM structures relating to present study are introduced in the following.

Javaheri and Eslami (2002a, b, c) and Shariat and Eslami (2007) reported mechanical and thermal buckling of rectangular functionally graded plates by using the classical plate theory and higher order shear deformation plate theory. They used energy method to derive governing equations that analytically solved to obtain the closed-form solutions of critical loading. The same authors and (Shariat et al., 2005; Shariat and Eslami, 2006) extended their studies when influences of initial geometrical imperfection on the critical buckling loading are taken into consideration. Bouazza et al. (2010) used the first-order shear deformation theory to derive closed-form relations for buckling temperature difference of simply supported moderately thick rectangular power-law (linear, quadratic, cubic, and inverse quadratic) functionally graded plates. Buckling analysis of isotropic rectangular plates on elastic foundation was carried out by Yu (2008). He considered a plate resting on elastic foundation with two opposite edges simply supported and different boundary conditions along the other edges (Levy
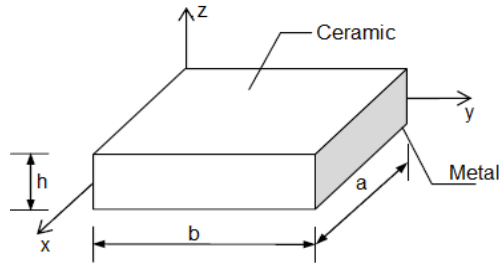
*Corresponding author. E-mail: bouazza_mokhtar@yahoo.fr.

Figure 1. Typical FGM rectangular plate.

solution). It was concluded that the number of waves of the buckling mode increases with stiffness and occurs in the direction of the applied stress. Also, increase in the plate width or height increases the buckling load for the free horizontal edge case, but the effect is the opposite for the clamped or simply supported cases. Hosseini-Hashemi et al. (2008) obtained an exact solution for the buckling of isotropic rectangular Mindlin plates. They considered a combination of six different boundary conditions in which two opposite edges are simply supported. Monoaxial in-plane compressive loads on both directions were considered as well as equal biaxial compressive loads. They presented the non-dimensional critical buckling loads and mode shapes for the six cases analyzed. Saidi et al. (2009) studied the axisymmetric bending and buckling analysis of thick functionally graded circular plates. They used unconstrained third order shear deformation plate theory for their analysis. An approximate method for simultaneous modification of natural frequencies and buckling loads was presented by Mirzaeifar et al. (2009). They obtained the first and second order derivatives of natural frequencies and buckling loads with respect to an arbitrary geometrical or physical property of a plate. Mohammadi et al. (2009) investigated the buckling behavior of functionally graded material plate under different loading conditions based on the classical plate theory (Levy solution); the governing equations are obtained for functionally graded rectangular plates using the principle of minimum total potential energy. An analytical approach for the elastic stability of simply supported rectangular plates under arbitrary external loads was proposed by Liu and Pavlovic (2008). They considered several cases of buckling under direct, shear and bending loads.

The present article, the equilibrium and stability equations for FGM are obtained on the basis of classic plate theory and Navier's solution. Resulting equations are employed to obtain the closed-form solutions for the critical buckling load. The results are compared with the results of previous works in the literature.

FUNCTIONALLY GRADED MATERIALS

Consider a case when FGM plate is made up of a mixture of ceramic and metal as shown in Figure 1. The material

properties vary continuously across the thickness according to the following, which are the same as the equations proposed by Praveen and Reddy (1998):

$$E(z) = E_m + E_{cm} V_f(z) \qquad E_{cm} = E_c - E_m$$
$$\alpha(z) = \alpha_m + \alpha_{cm} V_f(z) \qquad \alpha_{cm} = \alpha_c - \alpha_m \tag{1}$$
$$\nu(z) = \nu_0$$

Where ν_0 Poisson's ratio of the plate is assumed to be constant through the thickness and subscripts m and c refer to properties of metal and ceramic, respectively, and $V_f(z)$ is volume fraction of the constituents which can mostly be defined by power–law functions (Chi and Chung, 2003a, b). For power-law FGM, volume fraction function is expressed as:

$$V_f(z) = \left(z/h + 1/2\right)^k \tag{2}$$

where E_m, α_m and E_c, α_c are the Young's modulus, coefficient of and the thermal expansion of the metal and ceramic surfaces of the FGMs plate, respectively.

GOVERNING EQUATIONS

This theory is based on the Cauchy, Poisson and Kirchhoff assumptions which maintain that the normal to the midplane before deformation remains normal after deformation. Then the displacement field in the (x; y; z) reference frame has the following form (Leissa, 1969):

$$U = u - zw_{,x} \qquad V = \upsilon - zw_{,y} \qquad W = w \tag{3}$$

where U, V and W are displacement components of a typical point in the plate, and $u; \upsilon$ are in-plane displacements at a point of the mid-plane.
Using the strain–displacement equations of the classical plate theory:

$$\varepsilon_x = U_{,x} \qquad \varepsilon_y = V_{,y} \qquad \gamma_{xy} = V_{,x} + U_{,y} \tag{4}$$

these kinematical equations can be written as

$$\varepsilon_x = \varepsilon_x^0 - zk_x \ ; \ \varepsilon_y = \varepsilon_y^0 - zk_y \ ; \ \gamma_{xy} = \gamma_{xy}^0 - zk_{xy} \tag{5}$$

where $\varepsilon_x^0, \varepsilon_y^0$ and γ_{xy}^0 are the mid-plane strains, and k_x, k_y and k_{xy} are the curvatures of the mid-plane during deformation. These are given by

$$\varepsilon_x^0 = u_{,x}, \quad \varepsilon_y^0 = \upsilon_{,y}, \ \gamma_{xy}^0 = u_{,y} + \upsilon_{,x}, \ k_x = w_{,xx} \quad , \ k_y = w_{,yy} \ , \ k_{xy} = 2w_{,xy} \tag{6}$$

Hooke's law for a plate is defined as

$$\sigma_x = \frac{E}{1-v^2}\left(\varepsilon_x + v\varepsilon_y - (1+v)\alpha T\right)$$

$$\sigma_y = \frac{E}{1-v^2}\left(\varepsilon_y + v\varepsilon_x - (1+v)\alpha T\right) \qquad (7)$$

$$\tau_{xy} = \frac{E}{2(1+v)}\gamma_{xy}$$

The forces and moments per unit length of the plate expressed in terms of the stress components through the thickness are

$$N_{ij} = \int_{-h/2}^{h/2}\sigma_{ij}\,dz \quad M_{ij} = \int_{-h/2}^{h/2}\sigma_{ij}z\,dz \qquad (8)$$

Substituting Equations 1 and 7 into Equation 8, gives the constitutive relations as

$$N_x = \frac{E_1}{1-v^2}(u_{,x}+vv_{,y}) + \frac{E_2}{1-v^2}(w_{,xx}+vw_{,yy}) - \frac{\Phi}{1-v}$$

$$N_y = \frac{E_1}{1-v^2}(vu_{,x}+v_{,y}) + \frac{E_2}{1-v^2}(vw_{,xx}+w_{,yy}) - \frac{\Phi}{1-v}$$

$$N_{xy} = \frac{E_1}{2(1+v)}(u_{,y}+v_{,x}) + \frac{E_2}{(1+v)}w_{,xy} \qquad (9)$$

$$M_x = \frac{E_2}{1-v^2}(u_{,x}+vv_{,y}) + \frac{E_3}{1-v^2}(w_{,xx}+vw_{,yy}) - \frac{\Theta}{1-v}$$

$$M_y = \frac{E_2}{1-v^2}(vu_{,x}+v_{,y}) + \frac{E_3}{1-v^2}(vw_{,xx}+w_{,yy}) - \frac{\Theta}{1-v}$$

$$M_{xy} = \frac{E_2}{2(1+v)}(u_{,y}+v_{,x}) + \frac{E_3}{2(1+v)}w_{,xy}$$

where

$$(E_1,E_2,E_3) = \int_{-h/2}^{h/2}(1,z,z^2)E(z)\,dz \quad (\Phi,\Theta) = \int_{-h/2}^{h/2}(1,z)E(z)\alpha(z)T(x,y,z)\,dz \qquad (10)$$

The equations of equilibrium for the plate are in the following form:

$$N_{x,xx} + 2N_{xy,xy} + N_{y,yy} = 0$$

$$M_{x,xx} + 2M_{xy,xy} + M_{y,yy} = 0 \qquad (11)$$

$$q + N_x w_{,xx} + N_y w_{,yy} + 2N_{xy}w_{,xy} = 0$$

Using Equations 9 and 10, the equilibrium in Equation 11 may be reduced to one equation as:

$$\nabla^4 w - \frac{1}{D}(N_x w_{,xx} + N_y w_{,yy} + 2N_{xy}w_{,xy} + q) = 0 \qquad (12)$$

where

$$D = \frac{E_1 E_3 - E_2^2}{E_1(1-v^2)} \qquad (13)$$

To establish the stability equations, the critical equilibrium method is used. Assuming that the state of stable equilibrium of a general plate under mechanical or thermal loads may be designated by w_0. The displacement of the neighboring state is $w_0 + w_1$, where w_1 is an arbitrarily small increment of displacement. Substituting $w_0 + w_1$ into Equation 12 and subtracting the original equation, results in the following stability equation:

$$\nabla^4 w_1 - \frac{1}{D}(N_x^0 w_{1,xx} + N_y^0 w_{1,yy} + 2N_{xy}^0 w_{1,xy}) = 0 \qquad (14)$$

where, N_x^0, N_y^0 and N_{xy}^0 refer to the pre-buckling force resultants.

For the solution of Equation 14, the Navier method is used. The displacement function is selected as the following Fourier series

$$w_1 = c\sum_{m=1}^{\infty}\sum_{n=1}^{\infty}\sin(m\pi x/a)\sin(n\pi y/b) \qquad (15)$$

where m, n are number of half waves in the x and y directions, respectively, and c is a constant coefficient.

MECHANICAL BUCKLING ANALYSIS

Consider a rectangular plate with the length a and width b which is subjected to in-plane loads as shown in Figure 2. Therefore, the pre-buckling forces can be obtained using the equilibrium conditions as (Mohammadi et al., 2009)

$$N_x^0 = \xi_1 P_1 \ , \ N_y^0 = \xi_2 P_1 \ , \ N_{xy}^0 = 0 \qquad (16)$$

where P_1 is the force per unit length, ξ_1 and ξ_2 are the load parameter which indicate the loading conditions. Negative values for ξ_1 and ξ_2 indicate that plate is subjected to biaxial compressive loads. Also, zero value for ξ_1 or ξ_2 shows uniaxial loading in x or y directions,
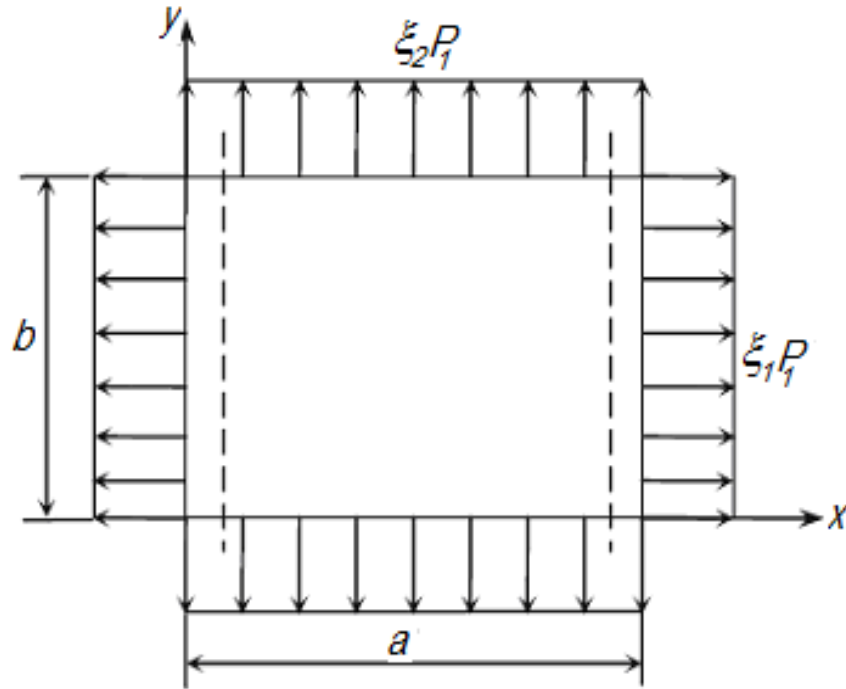
Figure 2. The rectangular plate subjected to in plane loads.

respectively. Substituting Equation 16 into Equation 14, one obtains

$$\nabla^4 w_1 - \frac{1}{D} P_1 \left(\xi_1 w_{1,xx} + \xi_2 w_{1,yy} \right) = 0 \tag{17}$$

Substituting Equation 15 into Equation 17, and substituting for the buckling load P_1

$$P_1 = -\frac{D\left[(m\pi/a)^4 + 2(m\pi/a)^2 (n\pi/b)^2 + (n\pi/b)^4 \right]}{\xi_1 (m\pi/a)^2 + \xi_2 (n\pi/b)^2} \tag{18}$$

The critical buckling load, P_{1cr}, is the smallest value of P_1 which is obtained when m = 1 and n = 1. Therefore,

$$P_{1cr} = -\frac{D\left[(\pi/a)^2 + (\pi/b)^2 \right]^2}{\xi_1 (\pi/a)^2 + \xi_2 (\pi/b)^2} \tag{19}$$

THERMAL BUCKLING ANALYSIS

In this section, the thermal buckling behaviors of fully simply supported rectangular metal-ceramic plates under thermal environment are analyzed. The thermal load

is assumed to be in uniform temperature rise and linear temperature rise through the thickness. The effects of volume fraction index and geometric parameter (a/b, a/h) are investigated in each case.

To determine the buckling temperature difference ΔT_{cr}, the pre-buckling thermal forces should be found firstly. Solving the membrane form of equilibrium equations gives the pre-buckling force resultants (Shariat and Eslami, 2007; Shariat and Eslami, 2005; Bouazza et al., 2010).

$$N_x^0 = -\frac{\Phi}{1-v}, \; N_y^0 = -\frac{\Phi}{1-v}, \; N_{xy}^0 = 0 \tag{20}$$

Substituting Equation 20 into Equation 14, one obtains:

$$\nabla^4 w_1 + \frac{1}{D} \frac{\Phi}{1-v} \nabla^2 w_1 = 0 \tag{21}$$

Uniform temperature rise

The plate initial temperature is assumed to be T_i. The temperature is uniformly raised to a final value T_f in which the plate buckles. The temperature change is $\Delta T = T_f - T_i$. Using Equations 1, 10, 15 and 21, the

buckling temperature change is obtained as:

$$\Phi = P\Delta T \tag{22}$$

Where

$$P = \int_{-h/2}^{h/2} E(z)\alpha(z)dz \tag{23}$$

The critical temperature difference is obtained for the values of m, n that make the preceding expression a minimum. Apparently, when minimization methods are used, critical temperature difference is obtained for m= n=1, thus

$$\Delta T_{cr} = \frac{D(1-\nu)\pi^2(1+B_a^2)}{a^2 P} \tag{24}$$

where

$$B_a = \frac{b}{a} \tag{25}$$

Linear temperature rise

The temperature field under linear temperature rise through the thickness is assumed as:

$$T(z) = \frac{\Delta T}{h}(z+h/2) + T_m \tag{26}$$

where z is the coordinate variable in the thickness direction which is measured from the middle plane of the plate.

T_m is the metal temperature and ΔT is the temperature difference between ceramic surface and metal surface, that is, $\Delta T = T_c - T_m$. For this loading case, the thermal parameter Φ can be expressed as

$$\Phi = PT_m + X\Delta T \tag{26}$$

Where

$$X = \int_{-h/2}^{h/2} E(z)\alpha(z)(z/h+1/2)dz \tag{27}$$

From Equation 26 one has

$$\Delta T = \frac{\Phi - PT_m}{X} \tag{28}$$

The critical buckling temperature change, ΔT_{cr}, is the smallest value of ΔT which is obtained when m = 1 and n = 1. Therefore,

$$\Delta T_{cr} = \frac{D(1-\nu)\pi^2(1+B_a^2)}{a^2 X} - \frac{PT_m}{X} \tag{29}$$

VALIDATION OF THE RESULTS

Based on the derived formulation, a computer program is developed to study the behavior of FGM plates in mechanical and thermal buckling. The analysis is performed for pure materials and different values of volume fraction exponent, k, for aluminium–alumina FGM. The Young's modulus and Poisson's ratio for aluminium are: 70 GPa and 0.3 and for alumina: 380GPa and 0.3, respectively. Note that the Poisson's ratio is chosen to be 0.3 for simplicity.

Mechanical buckling

In order to validate the results, a comparison with the known previous works has been carried out. In Table 1, the non-dimensional critical buckling load is presented in order to compare with results of Yu (2008) and Mohammadi et al. (2009) for an isotropic plate (k=0) with different aspect ratios. As table shows, the present results have a good agreement with results of Yu (2008) and Mohammadi et al. (2009).

On the other hand, to validate the derived equations, the obtained critical buckling load of simply supported FGM plates in Table 2 and the results of Mohammadi et al. (2009). They are in excellent agreement.

Thermal buckling

Uniform temperature rise

To validate the derived equations, the obtained critical buckling temperatures of simply supported isotropic plates subjected to a uniform temperature increase are compared with Boley and Weiner (1960), the results of Chen et al. (1991) and the results of Ganapathi and Touratier (1997) in Table 3. It can be seen that, for most cases the present results agree well with existing results.

Linear temperature rise

In addition, the buckling loads for simply supported, isotropic plates under linear temperature rise are calculated and compared in Table 4 with energy method results obtained by Kari et al. (1989) and finite element

Table 1. Comparison of the non-dimensional critical buckling load $(P_{1cr} \cdot a^2 / D)$ for an isotropic plate (k=0).

a/b	(ξ_1, ξ_2)	Yu (2008)	Mohammadi et al. (2009)	Present study
0.5	(-1,0)	15.42	15.4212	15.4213
	(-1,-1)	12.33	12.3370	12.3370
1	(-1,0)	39.23	39.4784	39.4784
	(-1,-1)	19.74	19.7392	19.7392

Table 2. Comparison of the critical buckling load (MN/m) for a FGM plate (b=1, h=0.01).

K	a/b	Critical buckling load					
		(ξ_1, ξ_2) =(-1,0)		(ξ_1, ξ_2) =(0,-1)		(ξ_1, ξ_2) =(-1,-1)	
		Mohammadi et al. (2009)	Present study	Mohamadi et al. (2009	Present study	Mohammadi et al. (2009	Present study
0	0.5	2.14655	2.14655	8.58619	8.58619	1.71724	1.71724
	1	1.37379	1.37379	1.37379	1.37379	0.68689	0.686896
	1.5	1.49066	1.61230	0.71658	0.71658	0.49609	0.49609
1	0.5	1.06993	1.06993	4.27971	4.27971	0.85594	0.85594
	1	0.68475	0.68475	0.6847532	0.68475	0.34238	0.34238
	1.5	0.74300	0.80363	0.35717	0.35717	0.24727	0.24727
2	0.5	0.83488	0.83488	3.33953	3.33953	0.66791	0.66791
	1	0.53432	0.53433	0.53432	0.53433	0.26716	0.26716
	1.5	0.57978	0.62709	0.27871	0.27871	0.19295	0.19295

Table 3. Comparison between the present solutions and results of Boley and Weiner (1960), Chen et al. (1991) and Ganapathi and Touratier (1997) for an isotropic plate.

Nondimensional critical buckling temperature for a simply supported isotropic plate				
E = 1, a/h = 100, $\nu = 0.3$, $\alpha = 1.0 \times 10^{-6}$				
a/b	Boley and Weiner (1960)	Chen et al. (1991)	Ganapathi and Touratier (1997)	Present
0.25	0.686	0.691	0.676	0.6722
0.50	0.808	0.814	0.798	0.7908
1.0	1.283	1.319	1.272	1.2653
1.50	2.073	2.101	2.072	2.0562
2.0	3.179	3.191	3.176	3.1633
2.5	4.599	4.601	4.585	4.5868
3.0	6.332	6.330	6.341	6.3267

using semiloof element results obtained by Gowda and Padalai (1970). They are in excellent agreement.

Results

Figure 3 shows the variation of the volume fractions of ceramic, in the thickness direction z for the functionally graded plate. The FGM plate considered here consists of aluminium and alumina. Figure 4 illustrates the variation of the critical buckling load of FGM versus the power of FGM, under different types of in-plane mechanical loading based on the classical plate theory. The thickness -to-side ratio h/a is assumed to be 0.01(a/b=1.25). It is shown that the critical buckling load

Table 4. Critical temperature for isotropic square plates subjected to linear temperature rise $\left(a/h=100,\alpha=2\cdot10^{-6},v=0.3\right)\cdot$

Temperature distribution	Analytical (Gowda and Padalai, 1970)	FEM (Kari et al., 1989)	Present
Linear temperature rise	126.54	126.00	126.5334
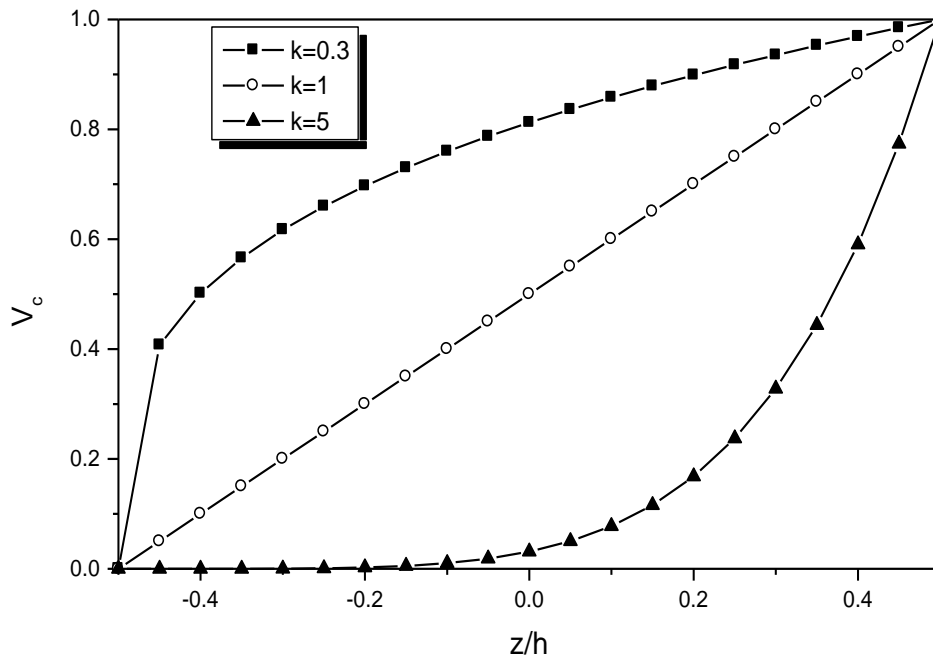
Figure 3. Volume fraction of ceramic along the thickness direction.
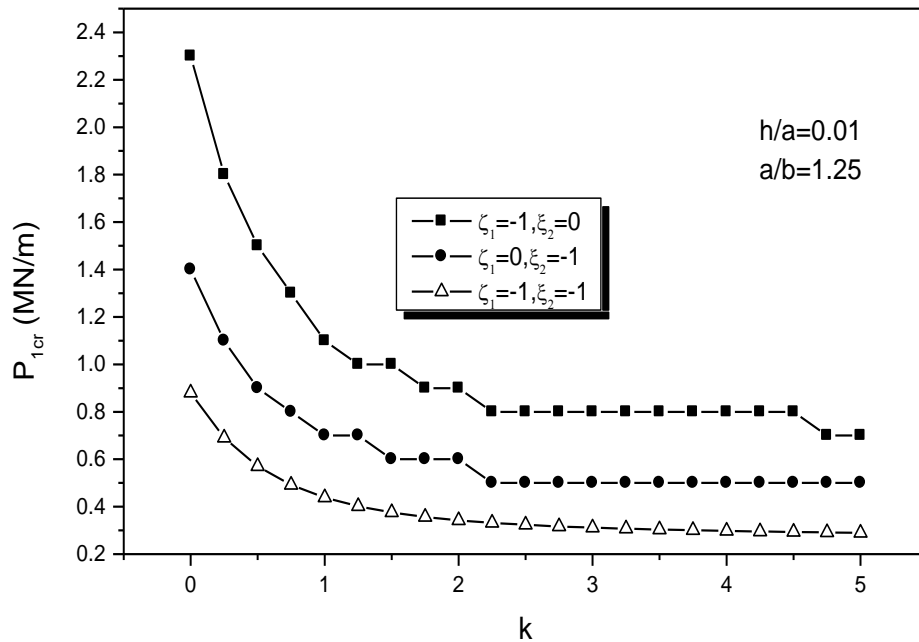
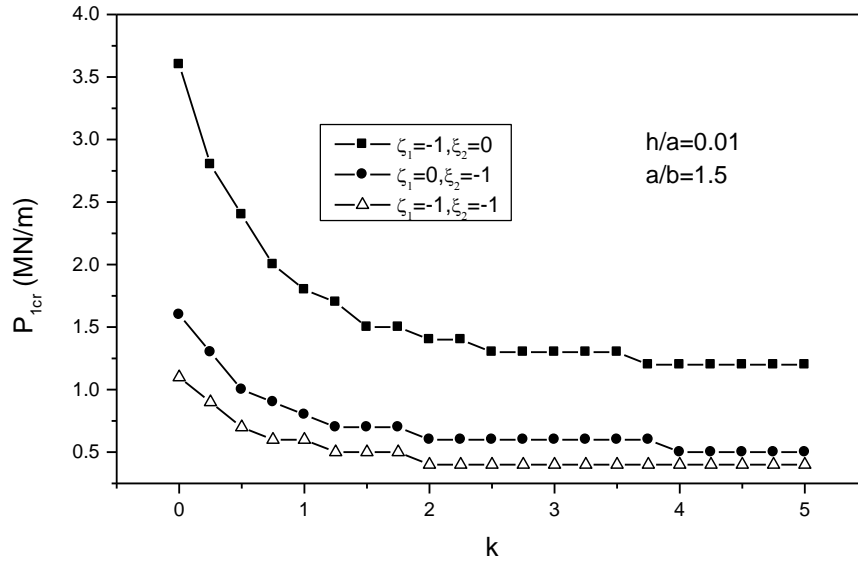**Figure 4.** Critical buckling load for a plate versus the power of FGM.

Figure 5. Critical buckling load for a plate versus the power of FGM.
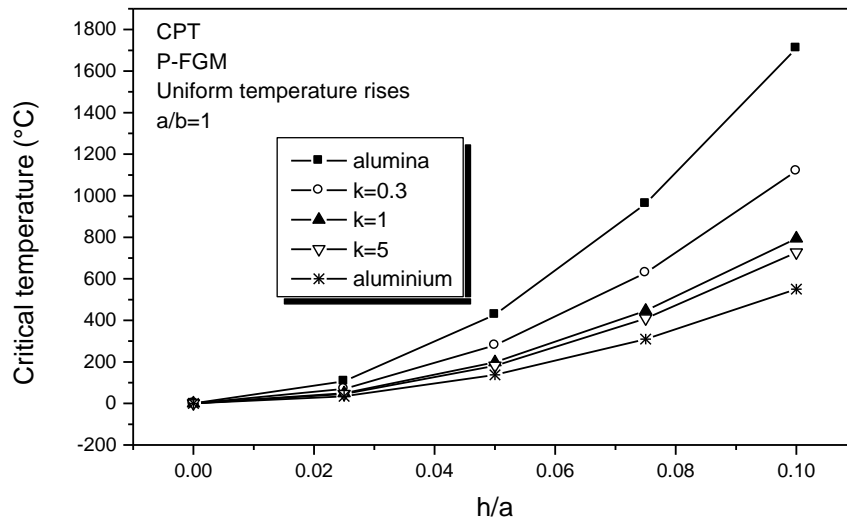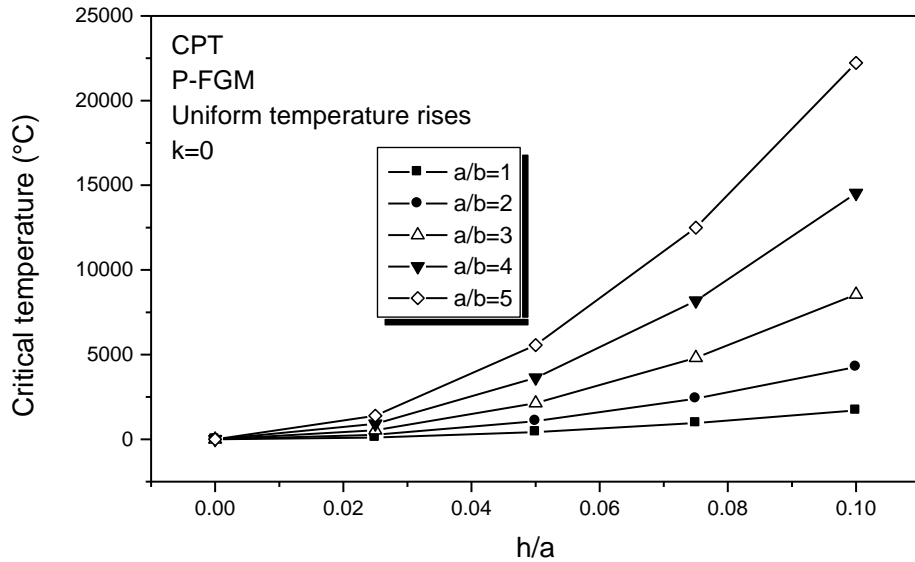

Figure 6. Critical buckling temperature of FGM plate under uniform temperature rise versus relative thickness of the plate with different values of k, using classic plate theory.

decreases as the power of FGM increases because high powers of FGM correspond to high portion of metal in comparison with the ceramic part. Also, the variation of critical buckling load is more apparent when the power of FGM is small. The buckling load of the plate under uniaxial compression is greater than the one under biaxial compression.

Figure 5 shows the critical buckling load P_{1cr} versus the power of FGM, under different types of in-plane mechanical loading based on the classical plate theory. The thickness-to-side ratio h/a is assumed to be

0.01(a/b=1.5). Comparing Figure 4 with Figure 5, the responses are nearly similar; however, the critical load change increases, when the geometric parameter a/b is increased. The variation of the critical temperature change ΔT_{cr} of aluminium-alumina FGM plates under uniform temperature rise for different geometric parameters and volume fraction index are plotted in Figures 6 and 7. The isotropic alumina and aluminium cases correspond to fully ceramic plates and fully metallic plates, respectively. While the other cases, $k = 0.3, 1, 5$, are for the graded plates with two constituent materials. In

Figure 7. Critical buckling temperature of FGM plate under uniform temperature rise versus relative thickness of the plate with different values of a/b, using classic plate theory.
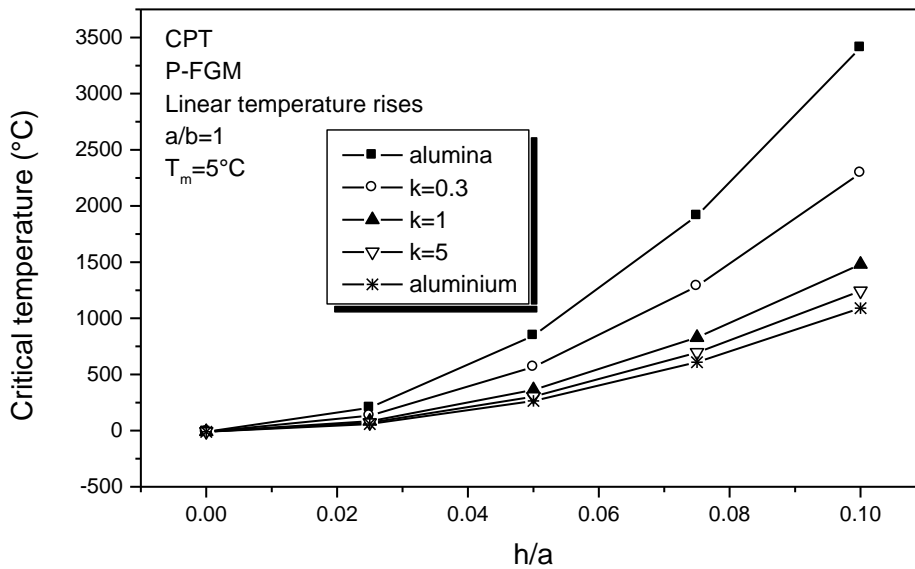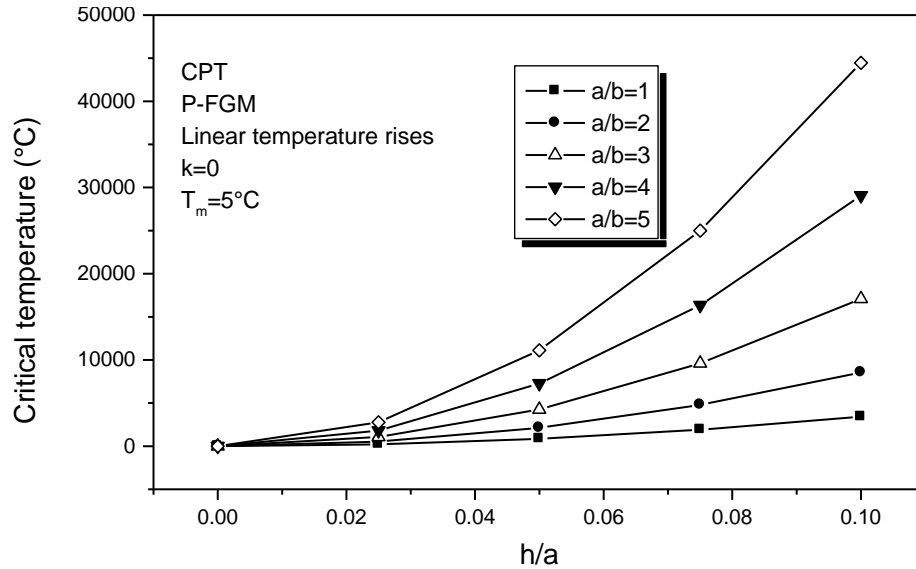

Figure 8. Critical buckling temperature of FGM plate under linear temperature rise versus relative thickness of the plate with different values of k, using classic plate theory.

Figure 6, it is found that the critical temperature change of FGM plates is higher than that of the fully metal plates but lower than that of the fully ceramic plates. In addition, the critical temperature change decreases as volume fraction index is increased. This is because for FGM, as the volume fraction index is increased, the contained quantity of metal increases. In all material cases, the critical temperature change increases, when the geometric parameter h/a is increased. On the other hand,

Figure 7 shows the critical temperature change increases, when the geometric parameter a/b is increased.

Figures 8 and 9 give the variation of the critical temperature gradient ΔT_{cr} of aluminium-alumina FGM plates under linear temperature rise. Comparing Figures 8 and 9 with Figures 6 and 7, the responses are very similar; however, the critical temperature gradient under

Figure 9. Critical buckling temperature of FGM plate under linear temperature rise versus relative thickness of the plate with different values of a/b, using classic plate theory.

linear temperature rise is higher than that under uniform temperature rise.

Conclusions

The buckling analyses of fully simply supported rectangular FGM plates under mechanical and thermal environment respectively are investigated by the classical plate theory. The mechanical loadings is assumed to be; uniaxial compression, and biaxial compression. The thermal load is assumed to be in uniform temperature rise and linear temperature rise. Based on the numerical results, the following conclusions are reached:

1. In the case of mechanical loads, the critical buckling mode varies with respect to the load parameter ξ_1 and ξ_2 or the aspect ratio a/b,
2. The buckling load of the plate under uniaxial compression is greater than the one under biaxial compression,
3. The critical buckling temperature for functionally graded rectangular plates are generally lower than the corresponding values for homogeneous plates made of ceramic. It is very important to check the strength of the functionally graded plate due to thermal buckling, although it has many advantages as a heat resistant material,
4. Geometric parameter h/a is increased, the critical temperature gradient increases rapidly,
5. Volume fraction index k is increased, the critical temperature gradient decreases. This is because as

volume fraction index is increased, the contained quantity of ceramic decreases,
6. The critical temperature under linear temperature rise is higher than that under uniform temperature rise.

REFERENCES

Boley BA, Weiner JJ (1960). Theory of Thermal Stresses. John Wiley, New York.

Bouazza M, Tounsi A, Adda-Bedia EA, Megueni A (2010). Thermoelastic stability analysis of functionally graded plates: An analytical approach . Elsevier, Comput. Mater. Sci. 49:865-870, ISSN 0927-0256.

Chen WJ, Lin FD, Chen LW (1991). Thermal Buckling Behavior Of Thick Composite Laminated Plates Under Nonuniform Temperature Distribution, Printed in Great Britain. Comput. Struct. 41(4):637-645.

Chi SH, Chung YL (2003a). Mechanical behavior of functionally graded material plates under transverse load-Part I: Analysis. Int. J. Solids Struct. 43:3657-3674.

Chi SH, Chung YL (2003b). Mechanical behavior of functionally graded material plates under transverse load- Part II: Numerical results. Int. J. Solids Struct. 43:3675-3691.

Ganapathi M, Touratier M (1997). A study on thermal postbuckling behaviour of laminated composite plates using a shear-flexible finite element. Finite Elem. Anal. Des. 28:115-135.

Gowda RMS, Padalai KAV (1970). Thermal buckling of orthotropic plates. In Studies in Structural Mechanics (Edited by K. A. V. Pa&alai), pp. 9-44. IIT, Madras.

Hosseini-Hashemi S, Khorshidi K, Amabili M (2008). Exact solution for linear buckling of rectangular Mindlin plates. J. Sound Vib. 315:318-342.

Javaheri R, Eslami MR (2002a). Buckling of functionally graded plates under in-plane compressive loading. ZAMM 82(4):277-283. Javaheri R, Eslami MR (2002b). Thermal buckling of functionally graded plates based on higher order theory. J. Therm. Stress. 25(1):603-625.

Javaheri R, Eslami MR (2002c). Thermal buckling of functionally graded plates. AIAA J. 40(1):162-169.

Kari R, Thangaratnam P, Ramachandran J (1989). Thermal buckling of composite laminated plates, Rimed in Great Britain. Comput. Struct. 32(5):1117-1124.

Leissa AW (1969). Vibration of plates. NASA, SP-160, Boley BA.

Liu YG, Pavlovic MN (2008). A generalized analytical approach to the buckling of simply supported rectangular plates under arbitrary loads. Eng. Struct. 30:1346-1359.

Mirzaeifar R, Shahab S, Bahai H (2009). An approximate method for simultaneous modification of natural frequencies and buckling loads of thin rectangular plates. Eng. Struct. 31:208-215.

Mohammadi M , Saidi A. R , Jomehzadeh E (2009). Levy Solution for Buckling Analysis of Functionally Graded Rectangular Plates. Int. J. Appl. Comp. Mater, DOI 10.1007/s10443-009-9100-z, Springer Science + Business Media B.V.

Praveen GN, Reddy JN (2006). Nonlinear transient thermoelastic analysis of functionally graded ceramic-metal plates. Int. J. Solids Struct. 35:4457-4476.

Saidi AR, Rasouli A, Sahraee S (2009). Axisymmetric bending and buckling analysis of thick functionally graded circular plates using unconstrained third order shear deformation plate theory. Compos. Struct. 89:110-119.

Shariat SBA, Eslami MR (2006). Thermal buckling of imperfect functionally graded plates. Int. J. Solids Struct. 43:4082-4096.

Shariat SBA, Eslami MR (2005a). Effect of initial imperfection on thermal buckling of functionally graded plates. J. Therm. Stress 28:1183-1198. Shariat SBA, Eslami MR (2007). Buckling of thick functionally graded plates under mechanical and thermal loads. Compos. Struct. 78:433-9.

Shariat SBA, Javaheri R, Eslami MR (2005b). Buckling of imperfect functionally graded plates under in-plane compressive loading. Thin-Wall Struct. 43:1020-1036.

Yu LH (2008). Buckling of rectangular plates on an elastic foundation using the Levy solution. AIAA. 46.